ELSEVIER

Journal of Molecular Catalysis A: Chemical 174 (2001) 193–204

JOURNAL OF MOLECULAR CATALYSIS A: CHEMICAL

www.elsevier.com/locate/molcata

Effect of second metals and Cu content on catalyst performance of Ni–Cu/SiO_2 in the hydrodechlorination of 1,1,2-trichloroethane into vinyl chloride monomer

Young Heon Choi, Wha Young Lee*

Division of Chemical Engineering, Seoul National University, Shinlim-dong, Kwanak-ku, Seoul 151-742, South Korea

Received 31 October 2000; received in revised form 21 January 2001; accepted 19 March 2001

Abstract

The hydrodechlorination of 1,1,2-trichloroethane (TCEA), which is one of the chlorinated organic wastes produced in the ethylene dichloride process, to vinyl chloride monomer (VCM) was carried out over Ni–Cu/SiO_2 catalysts. The effects of added metals from IB group and the Cu content on the performance of the bimetallic catalysts were systematically investigated. Of the screened bimetallic catalysts tested, Ni–Cu/SiO_2 catalysts efficiently converted TCEA into VCM in 95% or higher selectivity. Cu in Ni–Cu/SiO_2 reduced the metal particle size and weakened the adsorption strength of Ni, and led to low conversion of TCEA and a high VCM selectivity. A series of CO–IR and extended X-ray absorption fine structure (EXAFS) measurements revealed that added Cu had no effect on the electronic structure of Ni and that Cu altered the geometric nature of Ni–Cu/SiO_2 catalyst. HCl converted metallic Ni to $NiCl_2$ and Cu to CuCl to modify the crystal structure. Cu played a role in the cooperation with Ni in the hydrodechlorination of TCEA, serving as other than an inert spacer.

Keywords: Ni–Cu/SiO_2; Hydrodechlorination; 1,1,2-Trichloroethane; Vinyl chloride monomer; Metal particle size; Adsorption strength; HCl

1. Introduction

Considerable efforts have been made to eliminate chlorinated compounds from industrial waste streams. A number of approaches for reducing or eliminating chlorinated organic wastes include direct incineration [1], catalytic combustion [2], biodegradation [3], photo-catalytic decomposition [4], and catalytic hydrodechlorination [5]. Among these methods, the catalytic conversion of chlorinated organic wastes into useful hydrocarbons via hydrodechlorination is known as one of the more promising methods. In addition to environmental advantages, this process has obvious economic merits because the resulting hydrocarbons can be recovered and recycled. Therefore, the catalytic conversion of chlorinated hydrocarbons into valuable hydrocarbons by hydrogenolysis is a subject of considerable interest [6].

Studies of the hydrodechlorination of chloroalkanes have been mainly focused on the full conversion of chloroalkanes to alkanes [7–9]. Recently, however, new studies have been carried out to convert chloroalkanes into more useful unsaturated hydrocarbons [10–14]. Some investigators, who have examined the supported noble metal catalysts [10,11], concluded that the formation of the unsaturated hydrocarbons was considerably affected by the addition of second metal as a promoter. Metals from IB group were mainly tested as promoters [10,11]. Vadlamannati et al. reported that Cu content of Pt–Cu/C catalysts increased

* Corresponding author. Tel.: +82-2-880-7404; fax: +82-2-888-7295.
E-mail address: wyl@snu.ac.kr (W.Y. Lee).

1381-1169/01/$ – see front matter
PII: S1381-1169(01)00170-4

the ratio of ethylene/ethane [10] and similar results were reported by other workers [12]. The selective hydrodechlorination of 1,2-dichloroethane into ethylene was carried out using Pd–Ag/SiO_2 catalysts [11].

Other studies have also been carried out using Ni-loaded catalysts for the selective hydrodechlorination of chlorinated alkanes into alkenes [13,14]. Choi et al. [13] reported that 95% or higher selectivity could be achieved with Ni/SiO_2 catalyst in the hydrodechlorination of 1,2-dichloropropane to propylene.

However, the mechanism of formation of alkenes via the use of supported metal catalysts has not been clearly elucidated and the role of the added second metal remains a controversial issue [10,11].

In this study, the catalytic hydrodechlorination of 1,1,2-trichloroethane (TCEA), a major by-product of the ethylene dichloride (EDC) process, into vinyl chloride monomer (VCM) was carried out over Ni/SiO_2, Ni–Cu/SiO_2, Ni–Ag/SiO_2 and Ni–Au/SiO_2 catalysts in a continuous flow fixed-bed reactor. The effects of added metals from IB group (Cu, Ag and Au) and the role of Cu on the catalyst performance were intensively investigated. The prepared catalysts were characterized by X-ray diffraction (XRD), temperature programmed reduction (TPR), transmission electron microscopy (TEM), Fourier transform infrared spectroscopy (FT–IR), electron probe micro analyzer (EPMA), differential thermogravimetry (DTG), H_2 chemisorption, and extended X-ray absorption fine structure (EXAFS).

2. Experimental

2.1. Catalyst preparation

10Ni–5Cu/SiO_2, 10Ni–5Ag/SiO_2, 10Ni–5Au/SiO_2, and 10Ni/SiO_2 catalysts were prepared by co-impregnation of SiO_2 (Aerosil 200, surface area = 200 m^2/g, pore volume = 3.8 ml/g) with appropriate amounts of an aqueous solution of nickel nitrate ($Ni(NO_3)_2 \cdot 6H_2O$) and copper acetate ($Cu(NO_3)_2 \cdot 6H_2O$), silver nitrate ($AgNO_3$), and gold chloride ($AuCl_3$), respectively. After drying overnight at 393 K, the catalysts were calcined for 5 h at 723 K under a stream of air. The prepared bimetallic catalysts are referred to as xNi–yM/SiO_2, where x represents the wt.% of Ni loading and y represents the wt.% of the second metal loading. For example, 10Ni–5Cu/SiO_2 indicates that Ni loading on SiO_2 was 10 wt.% and that the Cu loading on SiO_2 was 5 wt.%.

2.2. Catalyst characterization

Catalysts were characterized by XRD, TPR, TEM, FT–IR, EPMA, DTG, H_2 chemisorption, and EXAFS.

The symmetry and crystallinity of the catalysts were confirmed by XRD (Rigaku, D/MAX-IIA), and peaks were assigned using JCPDS card files.

The TPR measurement was carried out in a conventional flow system in conjunction with a moisture trap connected to a thermal conductivity detector at temperatures ranging from room temperature to 1073 K with a heating rate of 5 K/min. The flow rate of the reducing gas was H_2 = 6 ml/min and N_2 = 34 ml/min for 0.1 g of catalyst.

The particle size and location of Ni on the catalyst surface was confirmed by TEM (Jeol, JXA-8900R) using an ultrasonically dispersed catalyst sample (in ethanol) deposited over a thin gold film.

IR spectroscopy of the adsorbed CO was measured in a chemisorption unit. The catalyst sample was pressed into a self-supporting thin wafer, placed at the center of the IR cell, vertically to the IR beam. The catalyst sample was reduced under a stream of hydrogen at 673 K for 2 h. After reduction, the sample was evacuated for 1 h at the same temperature, and cooled under vacuum (1×10^{-2} Torr) to the measurement temperature, 303 K and CO was then introduced into the cell (1 Torr, 303 K). IR spectra were obtained using a FT–IR (Bomem, MB-100).

Metal compositions on catalyst surface were measured by EPMA (JEOL, JXA-8900R).

Desorption behavior of TCEA on the catalysts was measured with DTG (Perkin-Elmer, thermo gravimetric analysis (TGA) 7) in a stream of nitrogen at a flow rate of 30 ml/min. The temperature was first raised to 373 K, maintained there for 1 h and then raised to 773 K at a heating rate of 10 K/min. Prior to the experiment, catalyst was reduced under flowing hydrogen at 673 K for 2 h, and cooled to the adsorption temperature, 423 K. Gas phase TCEA (3.64×10^{-2} mole) was fed to the catalyst under a stream of nitrogen, and purged with nitrogen for 5 h.

The chemisorption of hydrogen was measured in a chemisorption unit. A 0.2 g catalyst sample was placed in a glass U-tube sample holder and reduced

under a hydrogen flow at 673 K for 2 h. After the reduction, the sample was evacuated for 1 h at the temperature used for the reduction, and cooled under vacuum (1×10^{-4} Torr) to the measurement temperature, 293 K, and isotherms for total and irreversible adsorption were determined.

An X-ray absorption measurement was carried out, in order to investigate the state of metal above the Ni K edge and the Cu K edge at room temperature using beamline 3C1 at a Pohang light source.

2.3. Hydrodechlorination

The hydrodechlorination of TCEA into VCM was carried out in a continuous flow fixed-bed reactor at atmospheric pressure. The catalyst (100 mg) was charged in a tubular quartz reactor and activated in a stream of hydrogen (20 ml/min) and a nitrogen carrier (20 ml/min) at 673 K for 2 h. TCEA (3.64×10^{-3} mole/h) and hydrogen were then fed into the reactor, along with the nitrogen carrier (20 ml/min) for the reaction. The feed ratio of H_2/TCEA was 10. The reaction temperature was maintained at 573 K. The products were analyzed with FID in GC (HP 5890 II). A porapak Q was used as a column material**.**In all cases, the reaction was repeated under same conditions where rate and product reproducibility were within ±5%. Mass balance for the conversion of TCEA and the product selectivity was calculated in a carbon balance basis and it was confirmed by quantitative analysis of reactant and products. Effects of heat transfer and external mass transfer were negligible in our reaction conditions (TCEA feed rate: 3.64×10^{-3} mole/h, *W/F*: 28 g/mole/h, where *W* is the weight of the activated catalysts and *F* is the molar flow rate of TCEA, overall space velocity: 244 h^{-1} and reaction temperature: 573 K).

3. Results and discussion

3.1. Effect of added second metals on Ni/SiO_2 catalysts in the hydrodechlorination of 1,1,2-trichloroethane

Many workers have studied the effect of the second metal in the bimetallic catalysts on the selective hydrodechlorination of chloroalkane to alkene [10–12,15,16]. Bimetallic catalysts consisting of noble metals from VIII group and metals from IB group such as Pt–Cu/C [10,12] and Pd–Ag/SiO_2 [11], Pd–Bi/C, Pd–Tl/C [15], or Pd–Ni/C [16] catalysts have been tested for this reaction using chloroalkanes, such as 1,2-dichloroethane, 1,2-dichloropropane, TCEA and 1,2,3-trichloropropane as the model reactants. Vadlamannati et al. [10] reported that added Cu on Pt/C diluted the Pt ensemble and suppressed the hydrogenolytic ability of Pt, leading to cleavage at the C–Cl bond and enhancing the desorption of the $^{\bullet}CH_2$–$CH_2{}^{\bullet}$ species to ethylene. Similar results were reported by Harley et al. [12]. Heinrichs et al. suggested that 1,2-dichloroethane was adsorbed selectively on the Ag surface, following which 1,2-dichloroethane was dechlorinated by Pd, and finally, the $^{\bullet}CH_2$–$CH_2{}^{\bullet}$ species was desorbed as ethylene [11]. However, the role of the second metal is somewhat ambiguous, and has not yet been elucidated.

In this study, 10Ni–5Cu/SiO_2, 10Ni–5Ag/SiO_2, 10Ni–5Au/SiO_2, and 10Ni/SiO_2 were prepared to investigate the catalytic activity and product distribution in the hydrodechlorination of TCEA.

Fig. 1 shows the XRD patterns of the prepared catalysts after calcination at 723 K for 5 h under a stream of air. Characteristic peaks of NiO (37.2, 43.2, 62.8,

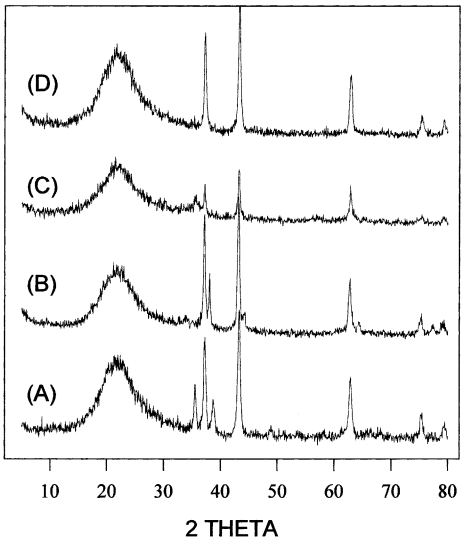

Fig. 1. XRD patterns of calcined catalysts with respect to second metals: (A) 10Ni–5Ag/SiO_2, (B) 10Ni–5Cu/SiO_2, (C) 10Ni–5Au/SiO_2, (D) 10Ni/SiO_2.

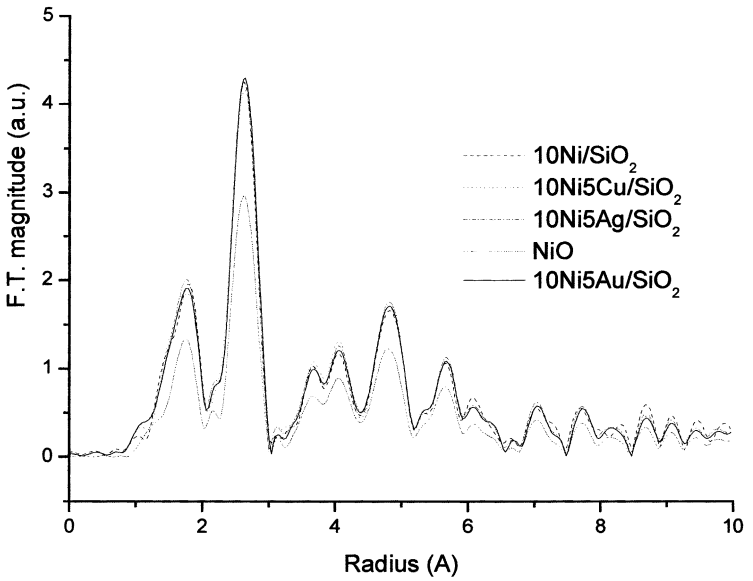

Fig. 2. Radial structure functions of calcined catalysts with respect to second metals measured by EXAFS at Ni K edge.

75.4, 79.4°) were observed for all catalysts, and peaks corresponding to metal–metal interaction were not observed. This phenomenon was confirmed by EXAFS.

Fig. 2 shows the radial distribution function profiles of the calcined catalysts measured by EXAFS above Ni K edge at room temperature. The profiles of all catalysts are nearly identical and they are very similar to that of NiO. This result indicates that NiO phase on catalyst was not affected by the added second metals.

Fig. 3 shows the TPR profiles of the prepared catalysts. Two broad peaks were observed between 600 and 900 K at 10Ni/SiO_2. The peaks between 600 and 700 K represent typical peaks for the reduced NiO [17] species supported on SiO_2, and the peaks appeared at higher temperatures are tentatively assigned to a nickel hydrosilicate [18]. This suggests that a metal–support interaction exists between nickel and SiO_2. The TPR profile of 10Ni–5Ag/SiO_2 showed two peaks. One is assigned to a reduction peak of AgO at 470 K and the other is due to the reduction peak of NiO at 560 K. The reduction temperature of NiO in the case of the 10Ni–5Ag/SiO_2 catalyst was lower than that of the other catalyst. This result suggests that the reducibility of Ni in 10Ni–5Ag/SiO_2 was enhanced with the addition of Ag. Two peaks are observed in the TPR profile of 10Ni–5Au/SiO_2. Since Au is easily reduced at room temperature [19], the two reduction profiles are tentatively assigned to the two collections of crystallites of different particle size [20]. Two reduction peaks are also observed in the case of 10Ni–5Cu/SiO_2. The peak at 510 K represents the reduction peak of CuO [20], and the broad peak at 600 K the reduction

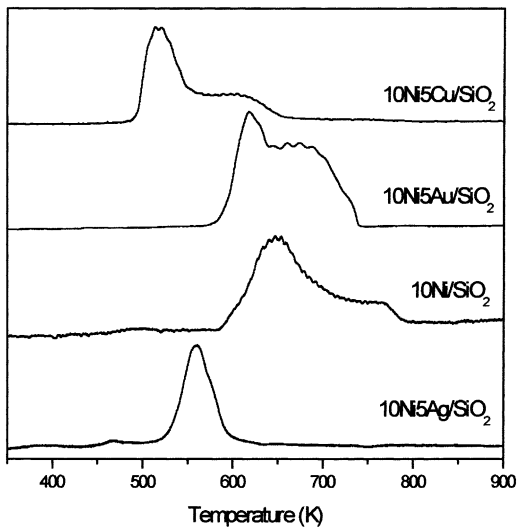

Fig. 3. TPR of calcined catalysts with respect to second metals.

peak of NiO. Added Cu produces spillover hydrogen which considerably accelerates the nucleation of the Ni metal in these reduction conditions, and enhances the reducibility of Ni [20].

Fig. 4 shows the conversion in the vapor phase hydrodechlorination of TCEA and product selectivity over Ni–metal/SiO_2 catalysts at 573 K with respect to the time on stream. The major products were VCM and ethylene for all catalysts. Small amounts of dichloroethylene and propylene were formed in the reaction, and trace amounts of methane and ethane were also detected. The catalytic activity of 10Ni/SiO_2 was decreased by ca. 25% after a period of 10 h on stream, and it was also observed that the selectivity of VCM was increased and ethylene selectivity was decreased. This phenomenon can be explained by the suggested Scheme 1. Hydrodechlorination of TCEA is predominantly a series reaction and C–Cl bond cleavage occurs sequentially. Therefore, if catalytic activity is reduced, the conversion of VCM into ethylene decreases and, as a result, it leads to the decrease of ethylene

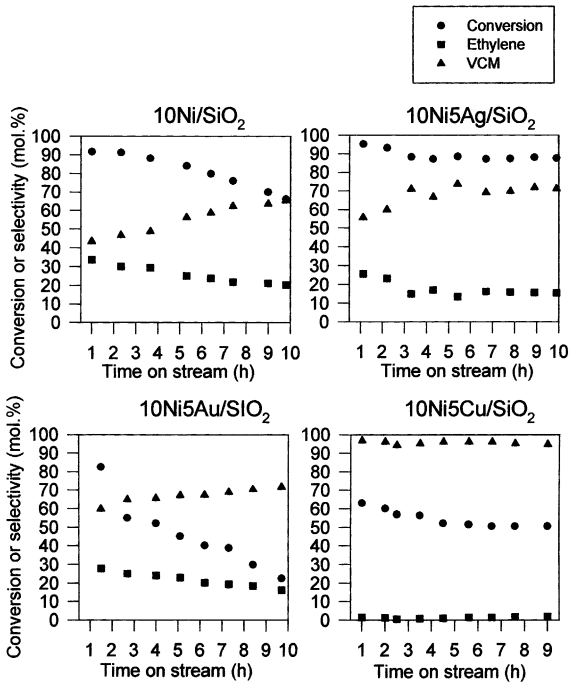

Fig. 4. Catalytic activity and product distribution of the Ni–metal/SiO_2 catalysts with respect to time on stream.

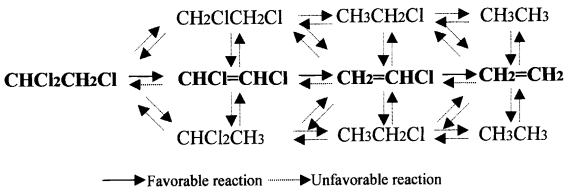

Scheme 1. Proposed reaction scheme for the selective hydrodechlorination of TCEA.

selectivity. The 10Ni–5Ag/SiO_2 catalyst showed the high conversion and at the same time low deactivation of catalyst. Product distribution of VCM and ethylene was similar to that of 10Ni/SiO_2. However, the product selectivities remained nearly constant for periods of up to 5 h. In case of the 10Ni–5Au/SiO_2 catalyst, although the initial activity was high, catalyst deactivation was severe. The catalytic activity and product distribution of 10Ni–5Cu/SiO_2 was somewhat different from that of other catalysts. Although the initial activity was lower than that of other catalyst, it remained nearly constant after 5 h, and 10Ni–5Cu/SiO_2 showed 95% or higher selectivity to VCM. A small amount of ethylene was formed. This result can be explained by two facts. One is due to the particle size of Ni. The dependency of the metal particle size on catalytic activity in the hydrodechlorination has been studied. It has been reported that large metal particle of catalysts enhanced the catalytic activity [14,21,22]. Fig. 5 shows the TEM results of the reduced catalysts. Although it is very difficult to distinguish Ni particle size from TEM data of bimetallic catalysts, the metal size of 10Ni–5Ag/SiO_2 and 10Ni/SiO_2 was clearly larger than that of 10Ni–5Cu/SiO_2 or 10Ni–5Au/SiO_2. They showed a higher activity. Added Cu or Au diluted the Ni ensemble and decreased the hydrogenolysis activity of Ni, leading to cleavage of the C–Cl bond [10]. The other one is due to the desorption behavior of TCEA on a reduced catalyst surface. TCEA was adsorbed on each catalyst in a TGA unit and desorption rate was measured at the temperature ranging from a room temperature to 800 K. Fig. 6 shows DTG profiles of the TCEA desorption from each catalyst. Two peaks are observed in the case of 10Ni–5Cu/SiO_2. The peak at 446 K can be attributed to the desorption of TCEA on the Cu metal and the peak at 524 K to the desorption of TCEA on the Ni metal. Added

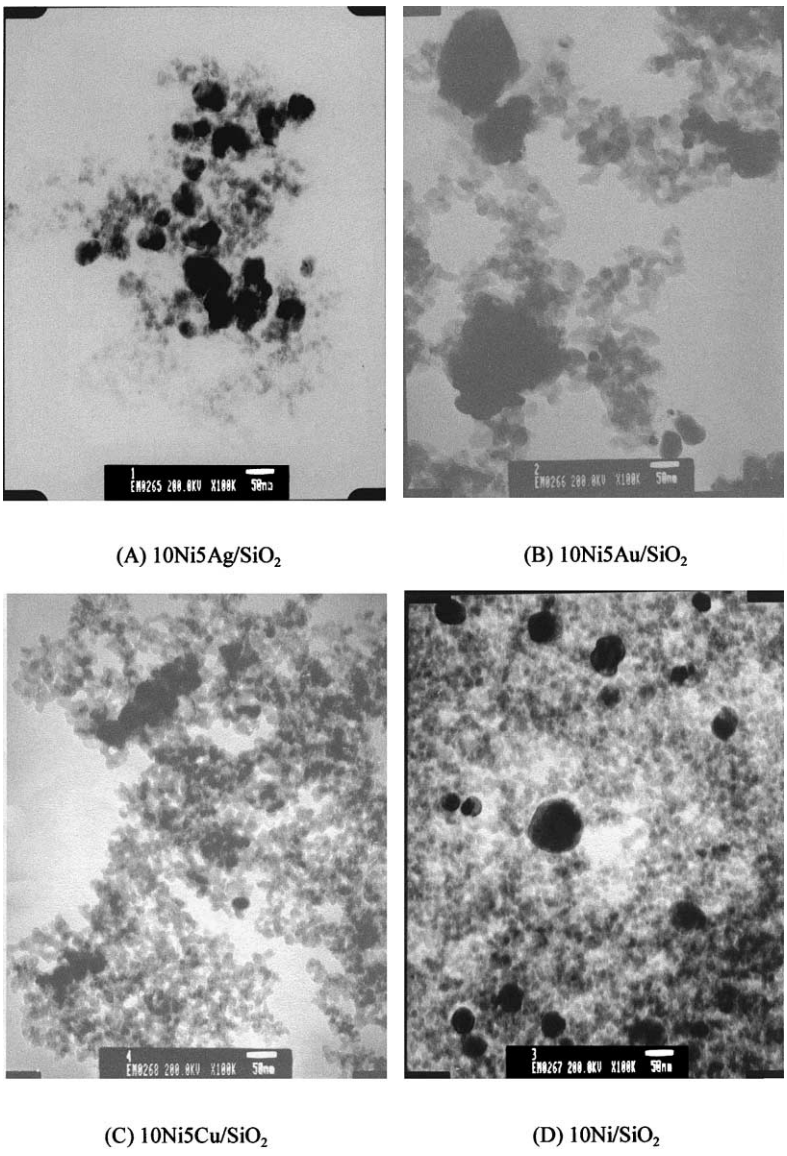

Fig. 5. TEM images of the reduced Ni–metal/SiO_2 catalysts.

Cu lowered the desorption temperature of TCEA on the Ni metal. The other catalysts showed only one broad desorption profile. The desorption temperature of TCEA on 10Ni–5Ag/SiO_2 is higher than that of the other catalysts. Therefore, it is presumed that TCEA on 10Ni–5Ag/SiO_2 is desorbed more slowly and as a result, further hydrodechlorination of TCEA occurs on 10Ni–5Ag/SiO_2. High selectivity to VCM and low conversion of TCEA on 10Ni–5Cu/SiO_2 can be also explained by desorption behavior. TCEA desorption which occurs readily on the metal surface by addition of Cu leads to a low conversion of TCEA. In addition, it is tentatively concluded that Cu weakened the adsorption strength of Ni, so that VCM is desorbed more rapidly, rather than being converted into ethylene.

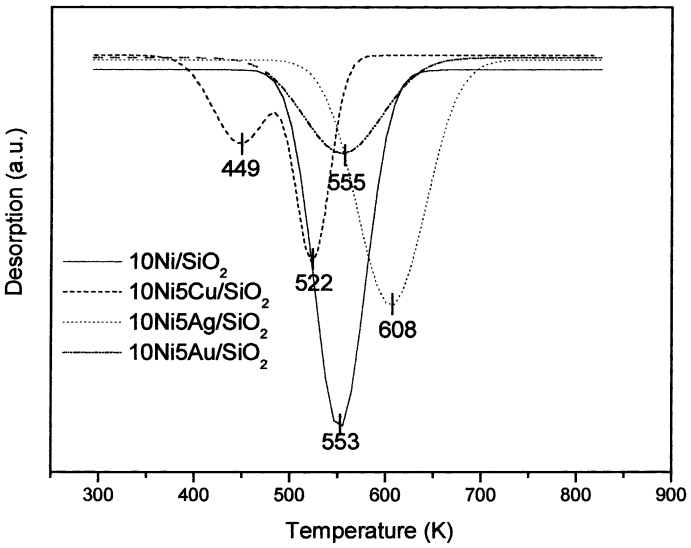

Fig. 6. DTG profiles of the Ni–metal/SiO_2 catalysts.

3.2. *Effect of Cu on Ni/SiO_2 catalysts in the hydrodechlorination of 1,1,2-trichloroethane*

Catalytic hydrodechlorination and characterization were intensively performed, in order to investigate the effect of Cu on Ni–Cu/SiO_2 catalysts. The characteristics of the prepared Ni–Cu/SiO_2 catalysts are listed in Table 1. The Ni/Cu atomic ratio at the surface was higher than that of the bulk composition of catalyst. As listed in Table 2, the rate of Ni diffusion is faster than that of Cu diffusion at low temperatures. Therefore, it is possible that Ni diffused more readily on the catalyst surface than Cu in the temperature range of 573–673 K, so that the Ni/Cu ratio at surface was relatively higher.

The Ni metal dispersion, which was measured by H_2 chemisorption, increased with increasing Cu content. This result suggests that Cu diluted the Ni ensemble.

Fig. 7 shows the XRD patterns of the reduced Ni–Cu/SiO_2 catalysts with respect to Cu content. Characteristic peaks for metallic Ni and Cu were observed and the intensity of the Cu peak increased with Cu content. However, in case of 10Ni–20Cu/SiO_2, a Ni peak was not detected in its XRD. This can be explained by the dilution effect of the Ni ensemble due to Cu and is consistent with the dispersion result.

Table 1
Characteristics of the prepared Ni–Cu/SiO_2 catalysts

Catalyst composition (wt.%)	Ni/Cu (bulk) (atomic ratio)	Ni/Cu[a] (surface) (atomic ratio)	Dispersion (%)[b]	Preparation method
SiO_2 support	–	–	–	
10Ni	∞	∞	13.20	Impregnation
10Ni + 1Cu	92/8	87/13	15.05	Co-impregnation
10Ni + 5Cu	68/32	74/26	16.51	Co-impregnation
10Ni + 10Cu	52/48	56/43	16.84	Co-impregnation
10Ni + 20Cu	35/65	43/56	17.10	Co-impregnation
10Cu	0/100	0/100	–	Impregnation

[a] Determined by EPMA.
[b] Determined by H_2 chemisorption.

Table 2
Diffusion rate of Ni and Cu as a function of temperature calculated by Fick's diffusion law [26]

Temperature (K)	Diffusion rate (cm^2/s)	
	Ni	Cu
373	1.91×10^{-22}	3.16×10^{-24}
473	1.22×10^{-18}	7.89×10^{-20}
573	3.19×10^{-16}	5.75×10^{-17}
673	1.69×10^{-14}	5.92×10^{-15}
773	3.22×10^{-13}	1.83×10^{-13}
873	3.12×10^{-12}	2.59×10^{-12}
973	1.89×10^{-11}	2.12×10^{-11}
1073	8.21×10^{-11}	1.17×10^{-10}
1173	2.77×10^{-10}	4.86×10^{-10}
1273	7.73×10^{-10}	1.61×10^{-9}
1373	1.86×10^{-9}	4.47×10^{-9}

Fig. 8 shows the XRD patterns of the Ni–Cu/SiO_2 catalysts as a function of Cu loading after a 10 h hydrodechlorination run. The XRD patterns of the used catalysts were different from those of the freshly reduced Ni–Cu/SiO_2 catalysts. Choi et al. [13] reported that HCl was formed during the hydrodechlorination, that HCl altered the crystal structure of the metallic nickel, and that nickel cubic structure was converted to a hexagonal symmetry (39.2, 41.5, 44.5, 58.3, 71.1 and 78.1°) during the reaction.

In addition, the characteristic peak for $NiCl_2$ at 15.2° ($NiCl_2$ (0 0 3)) was observed in the case of the used catalysts [13,23]. It was also observed that Cu metal was converted into CuCl phase (28.5, 47.4 and 56.2°).

In order to more precisely investigate the local structure of metals on catalysts, EXAFS measurements were carried out for the reduced and the used Ni–Cu/SiO_2 catalysts. Fig. 9 shows the radial structure functions of the reduced Ni–Cu/SiO_2 catalysts as a function of Cu loading at the Ni K edge. The main peak around 2.2 Å can be attributed to the interaction of Ni–Ni bond [24]. The Ni radial structure functions of the all catalysts except for 10Ni–20Cu/SiO_2 were shown to be very similar with that of Ni-foil. This in-

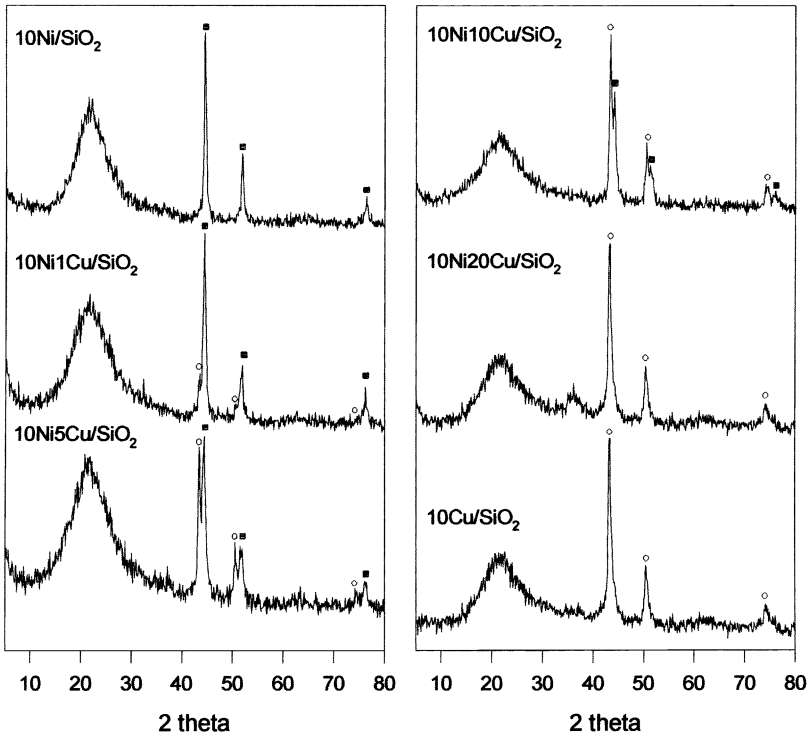

Fig. 7. XRD patterns of reduced Ni–Cu/SiO_2 catalysts as a function of Cu loading: (■) Ni (cubic), (○) Cu.

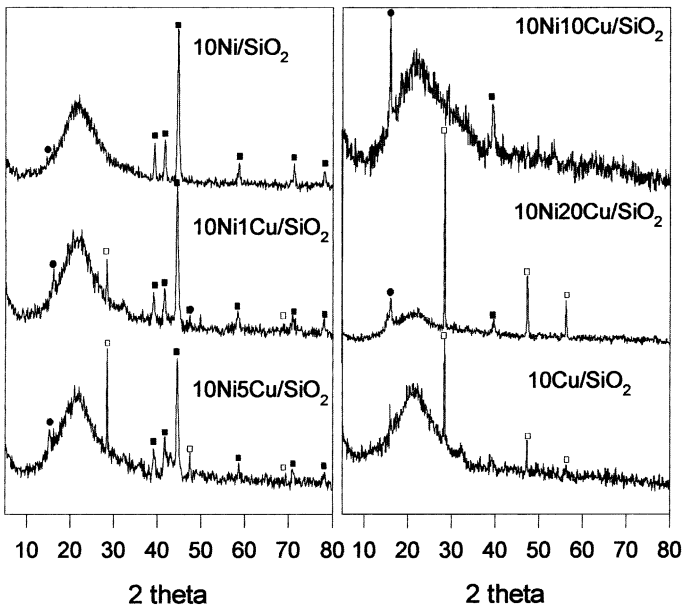

Fig. 8. XRD patterns of used Ni–Cu/SiO_2 catalysts as a function of Cu loading: (■) Ni (hexagonal), (●) $NiCl_2$, (□) CuCl.

dicates that the Ni component in reduced Ni–Cu/SiO_2 catalysts exists as pure Ni metal, and that the added Cu had little influence on the Ni phase. However, other peaks (1.2 and 1.6 Å) were observed in the 10Ni–20Cu/SiO_2 profile, and are presumed to be the peak generated by the interaction of Ni–Cu. Therefore, it can be inferred that a Ni phase with low Cu concentration on metal surface was not influenced by the Cu component, but if Cu on the metal surface is rich, it might influence the Ni phase and modify it. A

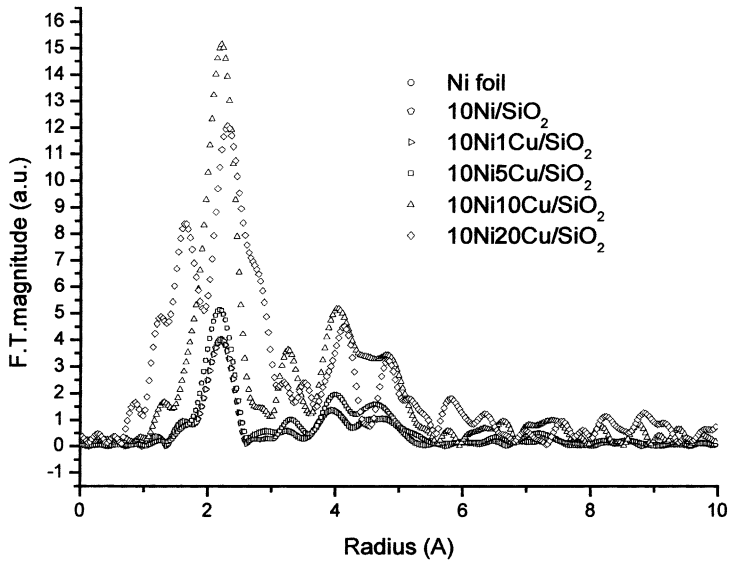

Fig. 9. Radial structure functions of the reduced Ni–Cu/SiO_2 catalysts as a function of Cu measured by EXAFS content at Ni K edge.

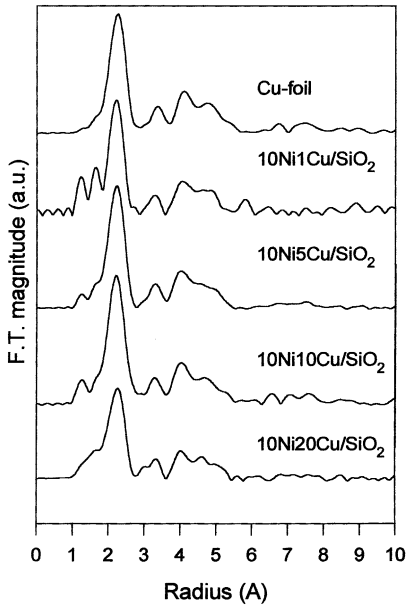

Fig. 10. Radial structure functions of the reduced Ni–Cu/SiO_2 catalysts as a function of Cu content at Cu K edge.

similar result is observed in the result of Ni–Cu/SiO_2 at Cu K edge, as shown in Fig. 10. When the Cu concentration was relatively low in comparison with Ni concentration, Cu phase was influenced by Ni. Hence, extra peaks are observed. However, the radial structure functions of Cu were similar to that of Cu-foil in high Cu concentrations.

Fig. 11 shows the radial structure functions of the used Ni–Cu/SiO_2 catalysts as a function of Cu loading at Ni K edge. Peak (A) is the profile of Ni-foil and peak (B) shows the radial structure function of $NiCl_2$. The first shell at ca. 1.6 Å represents the profile of $NiCl_2$ and can be attributed to an interaction of the Ni–Cl bond. Although a small peak of Ni–Cl bond was observed in 10Ni/SiO_2, the Ni phase was present as metallic Ni. However, in the case of Ni–Cu/SiO_2 catalysts, a peak at 1.6 Å was mainly observed. This indicates that Ni was mostly converted into $NiCl_2$ in the Ni–Cu/SiO_2 catalysts. It is in good agreement with the XRD results. The radial structure functions of the used Ni–Cu/SiO_2 catalysts at the Cu K edge are shown in Fig. 12. The Cu phase of the used catalysts showed two peaks at 1.5 and 2.8 Å. They are believed to be the peaks of CuCl, which can support the XRD results of the used catalysts. It was found from the XRD and EXAFS experiment that HCl modified the metallic Ni and Cu phases, converting them to $NiCl_2$ and CuCl, respectively.

The TPR profiles of Ni–Cu/SiO_2 catalysts as a function of Cu loading are shown in Fig. 13. It was observed from the profiles that reduction temperature of nickel oxide was lowered by the added Cu [20].

Fig. 14 shows the IR spectra of CO adsorbed on the Ni–Cu/SiO_2 catalysts at 1 Torr of CO pressure. In these spectra, two features can be distinguished, namely the high frequency bands (above 2000 cm^{-1}) and the low frequency bands (below 2000 cm^{-1}). The

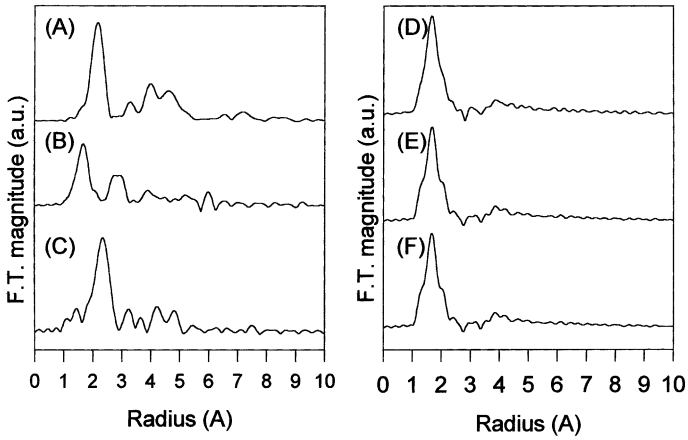

Fig. 11. Radial structure functions of used Ni–Cu/SiO_2 catalysts as a function of Cu content at the Ni K edge: (A) Ni-foil, (B) $NiCl_2$, (C) 10Ni/SiO_2, (D) 10Ni–1Cu/SiO_2, (E) 10Ni–5Cu/SiO_2, (F) 10Ni–10Cu/SiO_2.

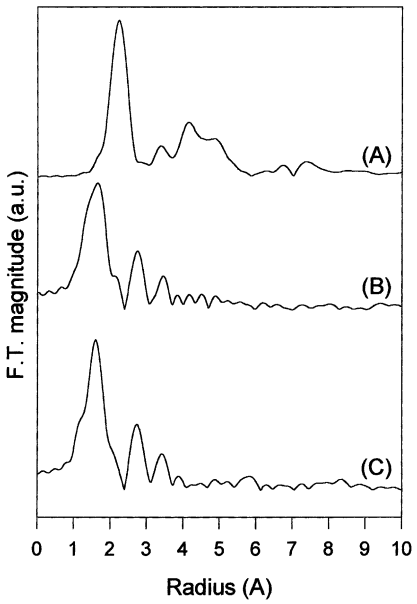

Fig. 12. Radial structure functions of used Ni–Cu/SiO_2 catalysts as a function of Cu content at the Cu K edge: (A) Cu-foil, (B) 10Ni–1Cu/SiO_2, (C) 10Ni–5Cu/SiO_2.

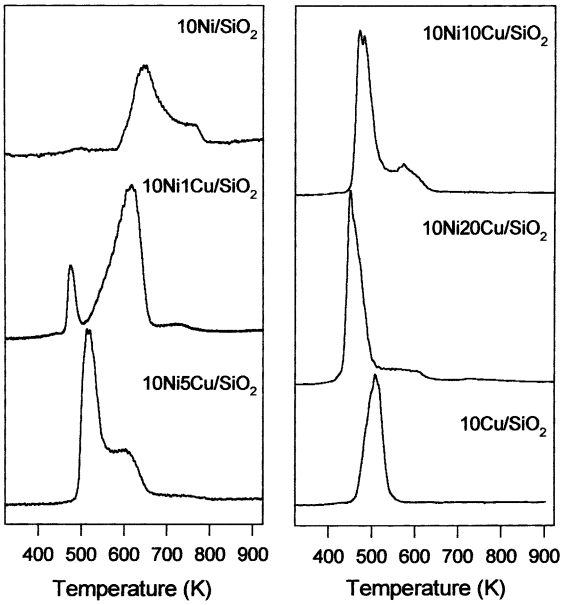

Fig. 13. TPR profiles of Ni–Cu/SiO_2 catalysts as a function of Cu loading.

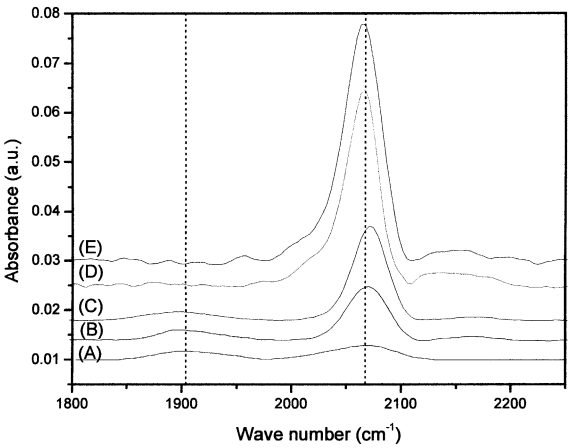

Fig. 14. FT–IR spectra of CO adsorbed on Ni–Cu/SiO_2 catalysts as a function of Cu loading: (A) 10Ni/SiO_2, (B) 10Ni–1Cu/SiO_2, (C) 10Ni–5Cu/SiO_2, (D) 10Ni–10Cu/SiO_2, (E) 10Ni–20Cu/SiO_2.

high frequency band is due to a linear bonding of CO with Ni, while the low frequency band is due to bridge-bonding CO [25]. The absorbance of the high and low frequency bands are comparable in 10Ni/SiO_2 catalysts, but the low frequency bands decreased and the high frequency increased markedly with increasing Cu content. However, the frequencies of the CO bands on all catalysts were virtually unchanged with metal composition. In the study of CO–IR for Ni–Cu/SiO_2, Soma et al. [25] concluded that the strength of the Ni–CO bond was not so much affected by the neighbors of the Ni atom and that the intrinsic character of each Ni atom in the Ni–Cu alloy surface was not appreciably changed with the alloy composition. Therefore, it can be inferred from CO–IR and EXAFS that added Cu did not influence the electronic structure of Ni and that Cu changed the geometric conditions of the Ni–Cu/SiO_2 catalysts.

Fig. 15 shows the catalytic activity and VCM selectivity in the hydrodechlorination of TCEA on Ni–Cu/SiO_2 catalysts as a function of Cu loading. 10Ni/SiO_2 showed the highest activity. This result can be explained by the metal particle size [14,21,22]. Although Ni–Cu/SiO_2 showed lower activity, they showed very high VCM selectivity. The 10Ni–10Cu/SiO_2 catalyst (43 at.% of Cu) showed a higher activity than the other Ni–Cu/SiO_2 catalysts. This feature of the catalytic activity can be explained

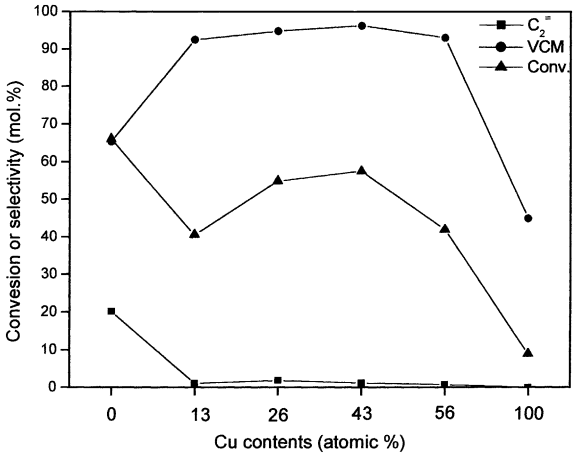

Fig. 15. Catalytic activity and product distribution of Ni–Cu/SiO_2 catalysts as a function of Cu at.% after a 10 h hydrodechlorination of TCEA.

by the role of Cu. Naturally, Cu added as a spacer decreased the Ni particle size and hydrodechlorination activity of Ni–Cu/SiO_2. However, Cu is capable of dechlorinating a chloroalkane to an alkene [10], although the catalytic activity of Cu is considerably lower than Ni. Therefore, in addition to Ni, Cu also might participate in the hydrodechlorination of TCEA and enhance the activity. The activity reduction of 10Ni–20Cu/SiO_2 catalyst (56 at.% of Cu) may be explained by the hypothesis that Cu diluted the Ni ensemble into a small size so that TCEA cannot be catalyzed, and abundant Cu on metal surface may hinder Ni from contacting the TCEA, leading to a low level of activity of the catalyst.

4. Conclusions

The hydrodechlorination of TCEA to VCM was carried out over Ni/SiO_2 catalyst modified with the metals from IB group in a continuous flow fixed-bed reactor. The effects of added metals on catalyst performance were intensively investigated. Of the screened bimetallic catalysts, Ni–Cu/SiO_2 catalysts efficiently converted TCEA into VCM in 95% or higher selectivity. It was found that Cu in Ni–Cu/SiO_2 reduced the metal particle size and weakened the adsorption strength of Ni, leading to a low conversion of TCEA and a high VCM selectivity. Added Cu had no influence on the electronic structure of Ni but changed the geometric conditions of Ni–Cu/SiO_2 catalyst. HCl converted the crystal structure of metallic Ni to $NiCl_2$ and Cu to CuCl. Cu played a role not as an only inert space but in cooperation with Ni in the hydrodechlorination of TCEA.

References

[1] J. Stach, V. Pekarek, R. Endrst, J. Hetflejs, Chemosphere 39 (1999) 2391.
[2] N. Coute, J.D. Ortego, J.T. Richardson, M.V. Twigg, Appl. Catal. B19 (1998) 175.
[3] D. Barrialt, M. Sylveste, Can. J. Microbiol. 39 (1993) 594.
[4] M. Trillas, J. Peral, X. Domenech, J. Chem. Tech. Biotechnol. 67 (1996) 237.
[5] A. Gampine, D.P. Eyman, J. Catal. 179 (1998) 315.
[6] D.J. Moon, M.H. Chung, K.Y. Park, S.I. Hong, Appl. Catal. A168 (1998) 159.
[7] S.P. Scott, T.J. Sweetman, A.G. Fitzgerald, E.J. Strurrock, J. Catal. 168 (1997) 501.
[8] B. Coq, J.M. Cognion, F. Figueras, D. Tournigant, J. Catal. 141 (1993) 21.
[9] K.A. Frankel, B.W.-L. Jang, G.W. Roberts, J.J. Spivey, Catalyst Deactivation, 1997, p. 239.
[10] L.S. Vadlamannati, V.I. Kovalchuk, J.L. d'Itri, Catal. Lett. 58 (1999) 173.
[11] B. Heinriches, P. Delhez, J. Schoebrechts, J. Pirard, J. Catal. 172 (1997) 322.
[12] A.D. Harley, T. Michael, D.D. Smith, M.D. Cisneros, US Patent 5,453,557.
[13] Y.H. Choi, W.Y. Lee, Catal. Lett. 67 (2000) 155.
[14] G. Tavoularis, M.A. Keane, Appl. Catal. A 182 (1999) 309.
[15] R. Ohnishi, W.L. Wang, M. Ichikawa, Appl. Catal. B 113 (1994) 29.
[16] C. Gervasutti, M. Venezia, US Patent 4,876,405.
[17] Y.C. Park, H.K. Rhee, Kor. J. Chem. Eng. 15 (1998) 411.
[18] J. van de Loosdrecht, A.M. van der Kraan, A.J. van Dillen, J.W. Geus, J. Catal. 170 (1997) 217.
[19] W. Juszczyk, Z. Karpinski, D. Lomot, J. Pielaszek, J.W. Sobczak, J. Catal. 151 (1995) 67.
[20] G. Ertl, H. Knozinger, J. Weitkamp (Ed.), Handbook of Heterogeneous Catalysis, VCH, Weinheim, 1997, p. 274.
[21] B. Coq, G. Ferrat, F. Figueras, J. Catal. 101 (1986) 434.
[22] W. Juszczyk, A. Malinowski, Z. Karpinski, Appl. Catal. B 166 (1998) 311.
[23] Y. Cesteros, P. Salagre, F. Medina, J.E. Sueiras, Appl. Catal. B 22 (1999) 135.
[24] J.C. Yang, Y.G. Shul, C. Louis, M. Che, Catal. Today 44 (1998) 315.
[25] Y. Soma, W.M.H. Sachtler, J. Catal. 34 (1974) 162.
[26] H. Schumann, Metallographie, Wilhelm-Pieck-Universität, Rostock, 1993.